References and Notes

(1) Olabisi, O.; Robeson, L. M.; Shaw, M. T. "Polymer-Polymer Miscibility"; Academic Press: New York, 1979.
(2) Bohn, L. *Rubber Chem. Technol.* **1968**, *41*, 495.
(3) Brode, G. L.; Koleske, J. V. *J. Macromol. Sci., Chem.* **1972**, *6* (6), 1109.
(4) Robeson, L. M.; Furtek, A. B. *J. Appl. Polym. Sci.* **1979**, *23*, 645.
(5) Seefried, C. G., Jr.; Koleske, J. V.; Critchfield, F. E. *Polym. Eng. Sci.* **1976**, *16*, 771.
(6) Paul, D. R.; Barlow, J. W. *J. Macromol. Sci., Rev. Macromol. Chem.* **1980**, *C18* (1), 109.
(7) Smith, K. L.; Winslow, A. E.; Petersen, D. E. *Ind. Eng. Chem.* **1959**, *51*, 1361.
(8) Osada, Y.; Sato, M. *J. Polym. Sci., Polym. Lett. Ed.* **1976**, *14*, 129.
(9) "Forming Association Compounds", F-43272, publication of Union Carbide Corp.
(10) Bank, M.; Leffingwell, L.; Thies, C. *Macromolecules* **1971**, *4*, 43.
(11) McMaster, L. P. *Macromolecules* **1973**, *6*, 760.
(12) Kwei, T. K.; Nishi, T.; Roberts, R. F. *Macromolecules* **1974**, *7*, 667.
(13) Nishi, T.; Wang, T. T.; Kwei, T. K. *Macromolecules* **1975**, *8*, 227.
(14) Nielsen, L. E. *Rev. Sci. Instrum.* **1951**, *22*, 690.
(15) Robeson, L. M. *J. Appl. Polym. Sci.* **1973**, *17*, 3607.
(16) Bailey, F. E.; Koleske, J. V. "Polyethylene Oxide"; Academic Press: New York, 1976.
(17) Koleske, J. V.; Lundberg, R. D. *J. Polym. Sci., Part A-2* **1969**, *7*, 795.
(18) Paul, D. R.; Barlow, J. W.; Cruz, C. A.; Mohn, R. N.; Wassar, T. R.; Wahrmund, D. C. *Org. Coat. Plast. Chem.* **1977**, *37* (1), 130.
(19) Gornich, F.; Hoffman, J. D. In "Nucleation Phenomena"; Michaels, A. S., Ed.; American Chemical Society: Washington, D.C., 1966; p 53.
(20) Hoffman, J. D.; Weeks, J. J. *J. Chem. Phys.* **1962**, *37*, 1723.
(21) Williams, M. L.; Landel, R. F.; Ferry, J. D. *J. Am. Chem. Soc.* **1955**, *77*, 3701.
(22) Robeson, L. M.; Joesten, B. L., paper presented at the New York Academy of Science, Oct 1975.
(23) Bortel, E.; Hodorowicz, S.; Lamot, R. *Makromol. Chem.* **1979**, *180*, 2491.

Excimer Formation in Dilute Solution. 1. Effect of Pressure on 1,3-Bis(2-naphthyl)propane and Poly(2-vinylnaphthalene)

Patrick D. Fitzgibbon and Curtis W. Frank*

Department of Chemical Engineering, Stanford University, Stanford, California 94305.

Received May 5, 1981

ABSTRACT: Excimer fluorescence is used as a probe of the bulk viscosity dependence of intramolecular segmental motion in dilute solution. The compounds studied are poly(2-vinylnaphthalene) (P2VN) of number-average molecular weight 300 000 and the dimer model compound 1,3-bis(2-naphthyl)propane ($\beta\beta$DNP). The viscosity of the toluene solvent is varied from 0.5 to 4.5 cP through application of hydrostatic pressures up to 450 MPa. The fluorescence behavior is analyzed in terms of Birks' scheme I kinetics for the photophysics and Kramers' theory for the segmental motion. The $\beta\beta$DNP data are fit satisfactorily by the Kramers treatment in the intermediate friction regime. The P2VN results, on the other hand, are fit better by the high-friction limit of the Kramers treatment, assuming that the effective local viscosity is different from the bulk solvent viscosity.

Introduction

The objective of this work is to examine intramolecular conformational rearrangement in dilute solutions of the aromatic vinyl polymers using excimer fluorescence as a molecular probe. Excimer formation in aromatic molecules is an important photophysical process which has been implicated in concentration quenching in solvents, in competitive excitation trapping in scintillator hosts, and as an intermediate step in photodegradation. Initial research efforts in the area were directed toward understanding the thermodynamics and kinetics of intermolecular excimer formation.[1,2] More recently, work has concentrated on the intramolecular process observed in model compounds and the aromatic vinyl polymers.[3]

Analysis of the photophysics of excimer formation in solution is complicated because sampling of suitable excimer-forming polymer chain conformations may result both from exciton migration and from rotational transformation due to solvent collision. Since only the second process is active in compounds containing two aromatic chromophores bound by a propane linkage, it may be possible to use information on these dimers to interpret excimer fluorescence in polymers. In this paper, 1,3-bis-(2-naphthyl)propane ($\beta\beta$DNP) is examined as such a model along with the corresponding polymer poly(2-vinylnaphthalene) (P2VN).

In most studies on the influence of bulk solvent viscosity on intramolecular excimer fluorescence, homologous solvent series[4] or solvent mixtures[5-8] have been used to achieve the viscosity variation. A possible difficulty in these approaches is that there may be large local variations in the solvent shell interactions with the isolated or complexed aromatic chromophores. Steric or specific chemical interactions between the solvent molecules and aromatic rings should affect both the rotational transformation process and the stability of the excimer complex once it is formed. This will be most significant when the solvents are chemically unrelated, as shown by Johnson.[4] To minimize this problem, hydrostatic pressure is used in this work to achieve a continuous variation in viscosity without changing the chemical character of the solvent shell. This variation can be appreciable; application of pressures to 450 MPa will cause the viscosity of toluene to increase from 0.5 to 4.5 cP.

The effect of pressure on intermolecular excimer formation has been the subject of several investigations.[9-17] These include studies on 1,2-benzanthracene, pyrene, perylene, and a number of naphthalene derivatives. The only pressure studies reported for intramolecular interactions have been on 1,3-bis(*N*-carbazoyl)propane.[13,14]

Experimental Section

A. Sample Preparation. 2-Ethylnaphthalene was obtained from Aldrich and used without further purification as a model compound for an isolated alkyl-substituted naphthalene ring, or monomer. 1,3-Bis(2-naphthyl)propane, the dimer model compound, was synthesized by a slight modification of the published

0024-9297/81/2214-1650$01.25/0

procedure[18] and was purified by column chromatography on silica gel. Poly(2-vinylnaphthalene) was synthesized in toluene solution using free radical polymerization initiated by azobis(isobutyronitrile) (AIBN). The 2-vinylnaphthalene monomer was purchased from Aldrich and purified by vacuum sublimation. The AIBN initiator was also purchased from Aldrich and purified by recrystallization in methanol. Toluene solvent was obtained from Fisher and distilled before use. The polymer was purified by multiple precipitation from toluene using Baker Photorex methanol as the nonsolvent.

The polymer molecular weight was determined by intrinsic viscosity measurements in toluene and by gel permeation chromatography (GPC) using a Waters Model 244 liquid chromatograph equipped with Waters 100, 500, 10^3, 10^4, 10^5, and 10^6 Å μ-Styragel columns. The GPC results indicated that the purification procedure had removed all but an insignificant amount of low molecular weight impurities.

The monomer, dimer, and polymer were examined in toluene solution. The 2-ethylnaphthylene solution was degassed by four freeze–pump–thaw cycles and sealed off at 10^{-4} torr in a 0.5-in.-diameter cylindrical quartz tube. Solutions for the pressure apparatus were degassed by purging with dry nitrogen for 20 min. All solutions were 10^{-4} M in naphthalene repeat units since the excimer to monomer quantum yield ratio, Φ_D/Φ_M, was independent of concentration below this value.

B. Pressure Apparatus and Spectrofluorimeter. The pressure cell was constructed of Carpenter Custom 455 stainless steel and was of cubic design with four window ports. Two cylindrical single-crystal sapphire windows (1.143-cm diameter, 0.914-cm length) were used at right angles for the fluorescence measurements. The optical path length through the sample solution to the center of the cell was 0.711 cm. The window seal was achieved with a deformable 99.999% aluminum gasket interspersed between the window face and polished backup plug. The backup plug seal was of conventional design using, in order, a Viton O-ring, Teflon, lead, and berylium copper washers and a hardened 455 stainless steel compression ring.

A Eurotherm Model 919 digital temperature controller and eight Hotwatt strip heaters ($1 \times 4 \times {}^3/_{32}$ in.) were used to keep the pressure cell at 30 ± 0.5 °C. The solution temperature within the pressure cell was monitored by an iron–constantan thermocouple which was pressure sealed in the same manner as the backup plug. A separator constructed of a 455 stainless steel cylinder having a brass piston with double O-ring seal was used to separate the sample solution from the Isopar-H hydraulic fluid of the pressure-generating system. The hydraulic system consisted of an Enerpac P-228 hand pump and a Harwood Engineering 10:1 intensifier (Model E-1985, B2.5). Maximum operating pressure was 65 000 psi (450 MPa).

The spectrofluorimeter was of modular design, consisting of a Schoeffel 1000-W xenon arc lamp, Schoeffel tandem ${}^1/_4$-m excitation monochromators, a stepper-motor-driven Schoeffel ${}^1/_4$-m analyzing monochromator, a thermoelectrically cooled EMI 9558 QB photomultiplier tube powered by an EMI 3000R high-voltage power supply, and an EMI 1012 picoammeter. The output from the picoammeter was sent to an ADVII-A 12-bit analog-to-digital converter in a PDP 11/03 remote microcomputer which was linked to a PDP 11/34 host minicomputer. The stepper motor on the analyzing monochromator could be driven either by the microcomputer or by a programmable pulse generator. The spectral response function of the spectrofluorimeter was obtained by using an Optronics Laboratories 200-W quartz–halogen Standard of Spectral Irradiance Model 220A powered by an Optronic Laboratories constant-current power supply, Model 65. The response function was determined by a method similar to that given by Parker.[19]

C. Data Analysis. Each spectrum consisted of 1000 time-averaged points spaced 0.25 nm apart. This was spectrally corrected using the instrumental response function and converted to an energy scale for subsequent analysis. All compounds were examined at 2500-psi increments, with reproducibility of the fitted spectral parameters at a given pressure being within 3%. After subtraction of the Raman and scattered light peaks, a nonlinear regression analysis utilizing the Marquardt method[20,21] was used to extract spectral parameters from the corrected emission envelopes. To minimize computation time, the spectra were fit to two functional forms. The first consisted of the entire vibrational envelope of the 2-ethylnaphthalene monomer; the second consisted of the excimer band, which has been predicted to be Gaussian in shape.[22] Although this was a good approximation for $\beta\beta$DNP, the middle of the monomeric portion of the P2VN spectra differed slightly from that for 2-ethylnaphthalene. In this case, the fitting was performed on only those points which were lower in energy than the high-energy half-height of the excimer peak. This procedure was compared with an analysis of the spectrum using one excimer and eight monomer Gaussians; no appreciable differences were detected.

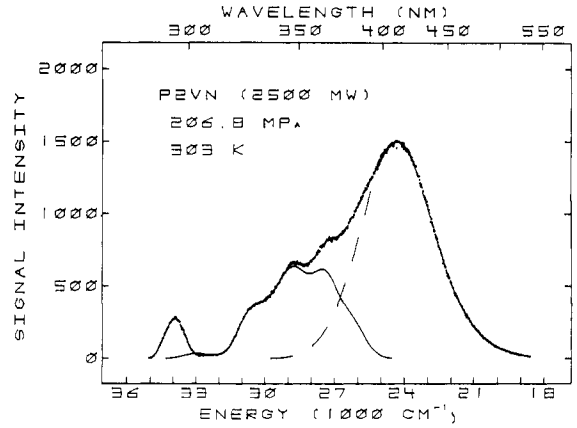

Figure 1. Typical corrected fluorescence spectrum showing regression fits. The dashed line is the fit of the excimer to a Gaussian peak shape and the solid line is the accompanying fit to the monomer vibronic manifold.

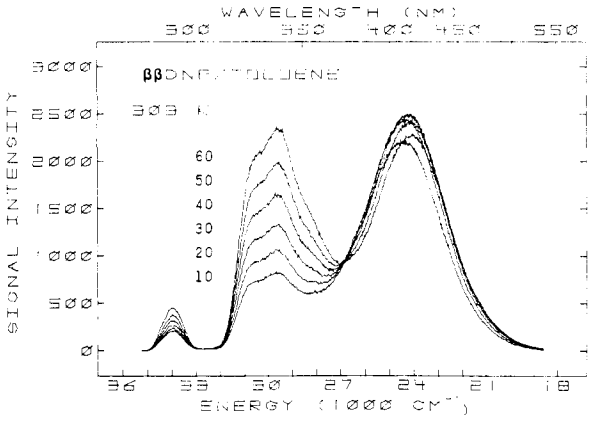

Figure 2. Pressure dependence of corrected spectra of $\beta\beta$DNP in toluene (10^{-4} M) at 30 °C. The numbers on the left indicate the pressure in units of 1000 psi for the corresponding fluorescence envelopes. Note the isoemissive point at 27 000 cm^{-1}.

Results

Corrected fluorescence spectra are shown in Figure 1–3. The monomer and excimer bands are identified in Figure 1, which shows a typical spectrum for a P2VN sample of M_n = 2500. The emission envelope consists of the time-averaged intensities recorded by the computer and corrected by the spectral response function. The band near 34 000 cm^{-1} results from incident light which is elastically scattered by the sample. The structured emission between 32 000 and 27 000 cm^{-1} is the monomer vibrational progression, with the solid line indicating the least-squares fit of the monomer envelope to eight Gaussians. The broad structureless band with maximum near 24 000 cm^{-1} is due to the excimer; the dashed line is the Gaussian fit of the excimer band which is compatible with the monomer spectrum. The effect of pressure on the corrected spectra of the $\beta\beta$DNP dimer and the P2VN (300 000) is illustrated in Figures 2 and 3. The most significant feature of these

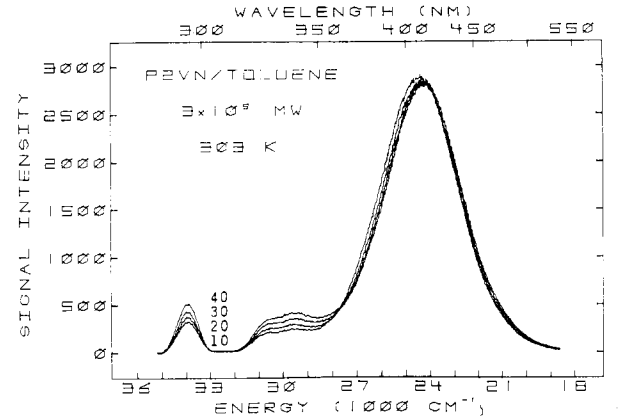

Figure 3. Pressure dependence of corrected spectra of P2VN with number-average molecular weight of 300 000. The isoemissive point is at 27 500 cm^{-1}.

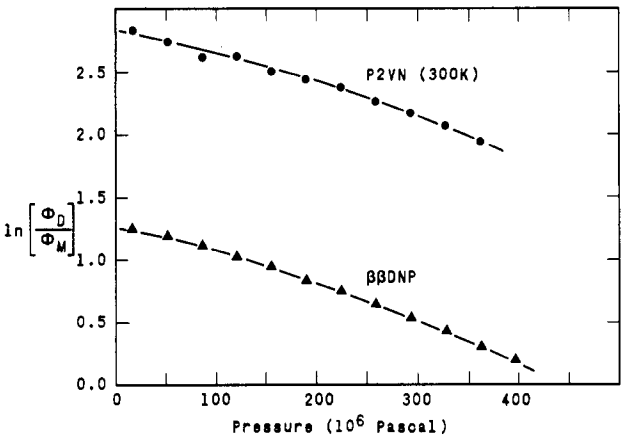

Figure 4. Variation of the excimer to monomer fluorescence quantum yield ratio, Φ_D/Φ_M, with pressure. (▲) ββDNP; (●) P2VN(300 000).

results is the existence of an isoemissive point for each compound, i.e., a particular wavelength at which the emission intensity is independent of the applied pressure.

The fluorescence measurements were made under photostationary state conditions. Experimental observables were all spectroscopic in nature, including the ratio of excimer to monomer emission quantum yields, Φ_D/Φ_M, the excimer band position, ν_D, and the excimer band width at half-height, $\Delta\nu_{1/2}$. The parameter of main interest is Φ_D/Φ_M, as determined from integrated area ratios; representative data are presented in Figure 4. There is a large difference between the initial Φ_D/Φ_M values for the two compounds, which is due to the additional contribution of energy migration to excimer sampling in the polymer. A more interesting feature of the results, at least for this study, is that Φ_D/Φ_M decreases with increasing pressure for both compounds. The excimer band position and width parameters, determined from the least-squares computer fits, are compiled in Table I.

Table I[a]

pressure		ββDNP		P2VN(300 000)	
10^3 psi	Mpa	ν_D	$\Delta\nu_{1/2}$	ν_D	$\Delta\nu_{1/2}$
5	34.5	24560	3790	24510	3790
10	69.0	24520	3790	24470	3790
20	137.9	24430	3760	24400	3790
30	413.7	24360	3770	24330	3790
40	275.8	24300	3760	24270	3780
50	344.8	24240	3750	24230	3790

[a] All excimer band positions and widths are given in units of cm^{-1}. The estimated errors are 50 cm^{-1} for ν_D and 30 for $\Delta\nu_{1/2}$.

Discussion

A. Excimer Photophysics. In the aromatic vinyl polymers there are three types of excimer-forming sites: intermolecular, intramolecular between rings on nonadjacent repeat units, and intramolecular between adjacent repeat units. At sufficiently high dilution, the intermolecular contribution may be eliminated entirely. Moreover, the population of nonadjacent intramolecular excimer sites should remain constant in a given solvent as the pressure is increased unless the thermodynamic properties of the solvent change. The only site of interest in this study is that occurring intramolecularly between adjacent repeat units.

The advantage of using intramolecular excimer fluorescence as a probe of motion in the polymer chain backbone is that stabilization of the excimer complex depends strongly upon the extent of π-orbital overlap between parallel apposed aromatic rings. Thus, the geometry is well defined. Flory has shown that the lowest energy conformational states in the vinyl polymers are the (g^+t, tg^-) states for a *dd* (meso) rotational dyad and (tt, g^+g^+) states for a *dl* (racemic) dyad.[23]. The corresponding excimer-forming states are (tt, g^-g^+) meso and (g^-t, tg^-) racemic.[24] Although the P2VN sample used in this work was atactic and the relative number of meso and racemic dyads is unknown, the latter should predominate in a free radically polymerized polymer.[25,26]

Although the conformational energy map for P2VN has not been determined, the statistical weight matrices should be very similar to those for polystyrene.[27] Calculations by Yoon et al.[28] on polystyrene show that racemic (g^-t, tg^-) conformations involve severe steric overlap between ortho hydrogens on the phenyl group and groups bonded to the next backbone α carbon and, thus, have energies more than 5 kcal/mol above the racemic tt minimum. The meso g^-g^+ is similarly of very high energy. The meso tt energy, on the other hand, is found to be approximately 1 kcal/mol above that of the meso tg minimum. Thus, the most likely excimer conformation is the tt meso dyad, which may be attained in the polymer by a single gauche–trans rotation from a preferred conformation. This conclusion is also supported by the excimer association rate data and energy maps on naphthalene dimer model compounds of Nishijima and Yamamoto.[29]

The situation is somewhat different for ββDNP, however, since it can be seen from the conformational energy map[29] that there should be a small additional contribution to excimer diffusional sampling due to rotations over two successive energy barriers. Such a multiple formation mechanism is consistent with the observation that the ββDNP excimer does not decay with a single exponential.[30] This additional process arises because the three-carbon backbone of ββDNP is more flexible than the polymer backbone.

The standard steady-state kinetic analysis due to Birks[1] yields the following expression for the ratio of excimer to monomer quantum yields:

$$R \equiv \frac{\Phi_D}{\Phi_M} = \left[\frac{k_{FD}}{k_{FM}}\right]\left[\frac{k_{rot}}{k_{FD} + k_{ID} + k_{MD}}\right] \quad (1)$$

where k_{FD} and k_{FM} are fluorescence decay rate constants for the excimer and monomer, k_{ID} is the rate constant for deactivation of the excimer complex by internal conversion, and k_{MD} is the rate constant for dissociation of the excimer to excited- and ground-state monomer. The rate constant

for association of an excited and unexcited aromatic ring leading to excimer formation has been denoted k_{DM} by Birks[1] but is here termed k_{rot} to emphasize the rotational diffusion process for intramolecular excimer formation. The use of eq 1 to analyze segmental motion is valid only if there is no other means of populating excimer sites. The trivial case of absorption at a preformed site is negligible due to the low equilibrium concentration of such conformations.[24] The sampling of excimer sites by energy transfer in the polymers is not negligible, however.

Incorporation of energy migration as an excimer site sampling mechanism in polymers is a difficult problem which is of considerable current interest.[31] It should be noted that the energy migration process does not create any new excimer sites. Rather, energy migration simply increases the probability that absorption of incident radiation by a pendant aromatic chromophore will lead eventually to excimer rather than monomer fluorescence. One simple way of formulating this concept is to incorporate a multiplicative enhancement factor E into eq 1.

$$R \equiv \frac{\Phi_D}{\Phi_M} = \left[\frac{k_{FD}}{k_{FM}}\right]\left[\frac{k_{rot}}{k_{FD} + k_{ID} + k_{MD}}\right]E \qquad (2)$$

Here, E is unity for the dimer model compound. From eq 2 it follows that the variation in Φ_D/Φ_M at atmospheric pressure is due simply to the increased effectiveness of energy migration in leading to excimer formation; i.e., E increases as the molecular weight of the polymer increases.

An implicit assumption in the use of hydrostatic pressure to vary the solvent viscosity is that pressure has no intrinsic effect on the exciton migration process. To isolate the energy migration mechanism, solid blends of 0.2% P2VN with polystyrene (PS) were prepared by solvent casting from benzene solution. Since the PS matrix is glassy at room temperature, the dispersed polymer cannot form excimers by segmental motion; only energy migration to preformed excimer sites will lead to excimer fluorescence. When the P2VN/PS solid film was subjected to hydrostatic pressure of up to 400 MPa, only a 10% decrease in Φ_D/Φ_M occurred. Thus, pressure has a negligible effect on the exciton migration and the decrease in Φ_D/Φ_M must be due mainly to the variation in segmental diffusion. It should be possible then to compare directly the backbone bond rotational behavior of a polymer with that of its dimer analogue.

Selinger and co-workers[10,12] have defined two limiting conditions with respect to eq 1 which encompass the pressure behavior of excimer formation for all aromatic molecules. In the first regime, denoted α, the rate of excimer dissociation to excited-state monomer is very fast with respect to deactivation by fluorescence or by internal conversion; i.e., $k_{MD} \gg k_{FD} + k_{ID}$. In this case, eq 2 reduces to

$$R \equiv \frac{\Phi_D}{\Phi_M} = \left[\frac{k_{FD}}{k_{FM}}\right]\left[\frac{k_{rot}}{k_{-D}}\right]E \qquad (3)$$

Here the ratio k_{FD}/k_{FM} is expected to be independent of pressure just as it is independent of solvent and temperature.[1] Since k_{rot} is the rate of formation of an excimer and k_{MD} is the rate of dissociation, the observed quantum yield ratio is proportional to the true molar equilibrium constant for excimer formation. This corresponds to Birks' "high-temperature dynamic equilibrium region".[1] Johnson[4] found that the rate constants for excimer association and dissociation have the same dependence on viscosity for 1,3-bis(*N*-carbazoyl)propane. Examination of results for 1,3-bis(1-naphthyl)propane[5] and for 1,3-bis(4-biphenyl)propane[32] leads to the same conclusion. Thus, it is probable that k_{rot}/k_{MD} will also be independent of viscosity for $\beta\beta$DNP. The factor k_{rot}/k_{MD} will, however, depend upon pressure. This dependence arises because excimer formation proceeds with a decrease in inter-ring separation distance; i.e., the activation volume for complex formation is negative. Since pressure will act to compress the complex and thus stabilize the excimer, k_{rot}/k_{MD} will increase with increasing pressure. This increase will lead to an increase in Φ_D/Φ_M with increasing pressure in the α regime.

The second limiting condition for eq 1, denoted β, occurs when the excimer dissociation rate is very slow with respect to deactivation; i.e., $k_{MD} \ll k_{FD} + k_{ID}$. Equation 2 then reduces to

$$R \equiv \frac{\Phi_D}{\Phi_M} = \left[\frac{k_{FD}}{k_{FM}}\right]\left[\frac{k_{rot}}{k_{FD} + k_{ID}}\right]E \qquad (4)$$

Here the fluorescence lifetime of the excimer, $\tau_D = 1/(k_{FD} + k_{ID})$, may be slightly pressure dependent, but, to a good approximation, Φ_D/Φ_M will be proportional to k_{rot}. Thus, excimer formation will depend upon viscosity, in contrast to the α limit. Since the rotational rate will decrease as the viscosity increases with increasing pressure, Φ_D/Φ_M will also decrease.

Whether or not excimer formation is viscosity dependent for any particular system depends upon the activation energy for dissociation and upon the absolute magnitude of the viscosity. Thus, at a constant temperature, a compound which is initially in condition α may transform to condition β as the viscosity increases due to application of pressure. Conversely, a transition from β to α may also occur if the pressure is maintained constant but the temperature is increased. The former behavior has been observed for intermolecular excimer formation in 1,2-benzanthracene[9,10] whereas the latter has been found in pyrene.[14,15]

An experimental indication that conditions are appropriate for either α or β behavior is the existence of an isoemissive point in the fluorescence spectra. Observations of isoemissive points resulting from variation in the solution temperature or in the concentration of aromatic substance have established that a necessary requirement for this behavior is that either $k_{MD} \gg k_{FD} + k_{ID}$ or $k_{MD} \ll k_{FD} + k_{ID}$.[33-36] The decrease in Φ_D/Φ_M with increasing pressure along with the presence of isoemissive points in Figures 2 and 3 indicates that both $\beta\beta$DNP and P2VN(300 000) are in the diffusion-controlled β region for all pressures indicated. At atmospheric pressure and 30 °C, however, they are in the intermediate region between pure dynamic equilibrium and pure diffusion control.

Although intramolecular rotational diffusion, as inferred from the Φ_D/Φ_M pressure dependence, is of primary interest for this work, some brief comments on the other spectroscopic parameters, particularly ν_D, are appropriate. From dielectric theory[37-40] it can be shown that a change in the dielectric constant of a continuous medium, ϵ, will result in a shift of the fluorescence envelope of a molecule embedded in that medium by an amount, $\Delta\nu_D$, which is proportional to the function $f(\epsilon) = (\epsilon - 1)/(2\epsilon + 1)$. In Figure 5 the shift in excimer band position with pressure for $\beta\beta$DNP and P2VN(300 000) is plotted against $f(\epsilon)$, where $f(\epsilon)$ has been evaluated by using data on the pressure dependence of the dielectric constant of toluene at 30 °C.[41] The slope of the dashed line was obtained by connecting the atmospheric-pressure values for the intermolecular excimer peak position of 2-methylnaphthalene in *n*-heptane[34] and in chloroform.[42] Both $\beta\beta$DNP and P2VN-

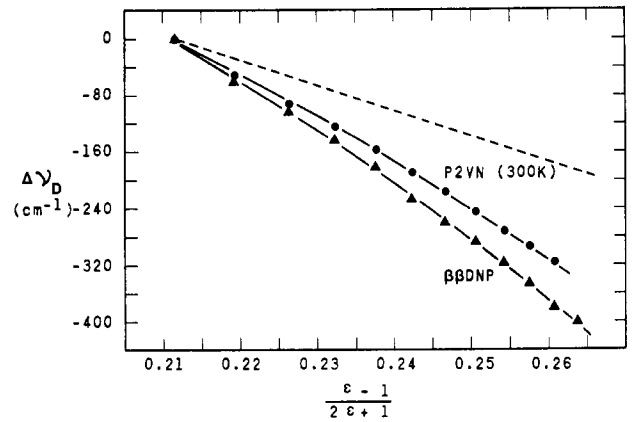

Figure 5. Variation of the excimer peak position with dielectric constant. The slope for the 2-methylnaphthalene intermolecular excimer is indicated by the dashed line. (▲) ββDNP; (●) P2VN(300 000).

(300 000) exhibit a larger excimer band shift than would be expected from the intermolecular results, indicating the pressure is acting to stabilize the excimer complex. Moreover, the excimer red shift is larger for the dimer than the polymer; i.e., the degree of stabilization is slightly higher. A possible explanation of this observation is that steric interactions between the excimer-forming rotational dyad and the adjacent backbone repeat units in the polymer prevent attainment of the same degree of overlap between rings as is possible in the dimer.

B. Previous Models for the Viscosity Dependence of Φ_D/Φ_M. Although a number of other investigators have recognized the potential of intramolecular excimer fluorescence as a probe of segmental motion, the analytical treatments have varied widely. It is of interest to review these briefly before developing the analysis of this work.

The simplest approach has been to assume that intramolecular excimer formation is a diffusion-controlled collision process identical with that observed for intermolecular association. In analyzing intermolecular excimer fluorescence resulting from concentration quenching of the emission from individual aromatic molecules, Birks[1] assumed that diffusion of ground- and excited-state monomer molecules could be treated by using Stokes' law. The rate constant for diffusion-controlled excimer formation was then found to be

$$k_{DM} = 8R_gT/3000\eta \tag{5}$$

where R_g is the gas constant and η is the solvent viscosity. Substitution of eq 5 for k_{rot} in eq 1 leads to an expression of the form

$$1/R = A_1'\eta \tag{6a}$$

or, equivalently,

$$R\eta = A_1 \tag{6b}$$

where $A_1 = 1/A_1'$ is a constant for a given solvent and temperature. It will be convenient to use the product $R\eta$ for comparing the different models since this product is independent of viscosity in the Birks model. Avouris[5] applied this approach to intramolecular excimer fluorescence from 1,3-bis(1-naphthyl)propane in ethanol–glycerol mixtures and found that at viscosities above 20 cP, eq 6a appeared to be applicable. A discrepancy exists in this treatment at low viscosity, however, because their $1/R$ vs. η plot did not extrapolate to zero at zero viscosity, as would be required.

This nonzero intercept can be explained by considering the effect of the connecting bonds on the relative rotational motion. A model which attempts specifically to incorporate these intramolecular restrictions to rotation is the "internal viscosity" approach of Peterlin.[43] In this model, the rate of conformational change is assumed to be of the form

$$k_{rot} = 1/(A_2' + A_3'\eta) \tag{7}$$

where A_2' and A_3' are constants. This treatment predicts that, at low viscosity, the rotational transformation rate depends primarily on the potential energy barrier represented by A_2' and is independent of viscosity, whereas the viscous hindrance term $A_3'\eta$ predominates at high viscosities. The fluorescence results should then follow

$$1/R = A_2 + A_3\eta \tag{8a}$$

or

$$R\eta = \eta/(A_2 + A_3\eta) \tag{8b}$$

where A_2 and A_3 are constants. This treatment was used by Morawetz and co-workers[6] in studies on dibenzyl ether, dibenzylamine, and their derivatives in ethanol–ethylene glycol–glycerol mixtures over the viscosity range from 1.8 to 53 cP. It is significant to note that eq 8 predicts that $R\eta$ becomes independent of η for large η and, thus, is consistent with the form of Avouris'[5] results.

Another model which incorporates the intramolecular restrictions to motion is based on Kramers' theory[44] for hindered motion over a potential barrier. Goldenberg et al.[7] attempted to explain their data on compounds of the generic type $ArCH_2XCH_2Ar$, where Ar is an aromatic moiety and X is either CH_2, O, or a nitrogen-containing group, by using the Kramers approach, with the friction factor being given by the Stokes formalism. Although they found that the expression they derived did not fit their results, the model presented in section C demonstrates the usefulness of the Kramers treatment for the pressure studies.

A fourth approach has been to emphasize the volumetric requirements for viscous transport of either solvent molecules or solute chain segments through the solvent. A liquid always has more empty space than the corresponding perfect crystal. This "free volume" is distributed randomly throughout the liquid in regions which vary considerably in size. In some locations, the equilibrium separation between nearest-neighbor solvent molecules may approach that for closest packing; in others, voids may exist which are larger than the solvent molecules. Viscous transport in the free volume model consists of two processes: sufficient free volume must first coalesce to form a void of appropriate size and then an adjoining solvent molecule must obtain sufficient energy to hop into the newly created cavity.

If the availability of free volume governs the rate of mutual solvent diffusion, the viscous solvent transport may be described by the Doolittle equation:[45]

$$\eta = \eta_0 \exp(\gamma/V_f) \tag{9}$$

where η_0 is a constant, γ is the effective volume required for viscous or diffusional motion, and V_f is the available free volume per molecule. Similarly, in a study of cis–trans isomerization, Gegiou[46] proposed a free volume limited reaction rate constant of the form

$$k = k_0 \exp(-\gamma'/V_f) \tag{10}$$

where k_0 is a constant. Here the exponential term could be interpreted as a Boltzmann factor for a reaction which requires an effective volume γ'.

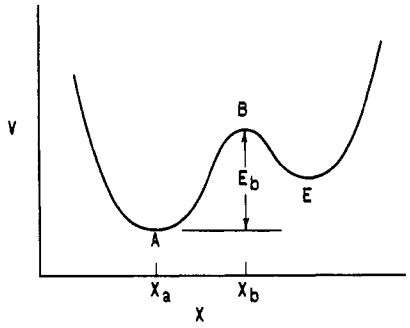

Figure 6. Potential energy diagram for hindered motions. Well A corresponds to the most probable conformation, barrier B of energy E_b relative to the minimum at A corresponds to an eclipsed conformation, and well E corresponds to the excimer conformation.

Johnson[4] adopted the physical analogy between internal isomerization and internal rotation leading to excimer fluorescence and developed an expression of the form

$$R = A_4\eta^{-\beta} \tag{11a}$$

or, equivalently,

$$R\eta = A_4\eta^{1-\beta} \tag{11b}$$

where A_4 is a constant.

In an extensive study of the rate constants for excimer formation and dissociation of 1,3-bis(*N*-carbazoyl)propane in a wide variety of related and unrelated solvents having viscosities between 0.2 and 20 cP, Johnson showed that eq 11a fit the results quite well as long as homologous solvent series were used. No agreement was found when solvents of widely differing chemical structure were used, however, implying that the solvent shell microstructure plays a significant role in the transport process. Bokobza et al.[47] found that eq 11 also fit their data for *meso*- and *dl*-2,4-diphenylpentanes and dibenzyl ether examined in mixtures of ethanol, ethylene glycol, and glycerol in which the viscosity varied from 1.8 to 53 cP.

From the preceding discussion, it should be clear that the specific question of the viscosity dependence of intramolecular excimer fluorescence is far from settled. Although it appears that $R\eta$ must be constant at high viscosity, the functional form at low viscosity depends upon whether availability of free volume or the energetics of internal rotation is more important. In the latter case, there seems to be sufficient ambiguity in the internal viscosity concept to warrant further examination. To this end, a model which emphasizes the hindered nature of intramolecular rotational motion is developed in section C. Subsequent comparison of each of the models with the experimental results is given in section D.

C. Hindered Rotational Motion in a Viscous Medium: Application of Kramers' Theory. If the major process leading to intramolecular excimer formation is assumed to be a single gauche–trans rotation, the theory of hindered motion in a viscous medium due to Kramers[44] should be relevant. This approach has been used by Helfand,[48-51] Blomberg,[52] Weber,[53] and Iwata[54] to explain polymer segmental mobility and should be directly applicable to the analysis of k_{rot}.

The assumed potential field for a hindered motion such as bond rotation past an eclipsed conformation is illustrated in Figure 6. The potential function at the minimum of the potential well, A, is assumed parabolic in the one-dimensional displacement

$$V_a = \frac{k_a}{2}(x - x_a)^2 \tag{12}$$

where k_a is the harmonic force constant. The oscillation frequency at the minimum is given by

$$\omega_a = \frac{1}{2\pi}\left(\frac{k_a}{M}\right)^{1/2} \tag{13}$$

where M is the reduced moment of inertia of the segment being moved by the bond rotation. The top of the barrier, B, is also considered to have parabolic shape

$$V_b = E_b - \frac{k_b}{2}(x - x_b)^2 \tag{14}$$

with barrier height E_b and force constant k_b, which is related to the oscillation frequency at the top of the barrier, ω_b, by an expression analogous to eq 13.

Kramers' theory requires that the particles in well A have an equilibrium Maxwellian distribution and, thus, that $\exp(-E_b/R_gT) \ll 1$. In a low-temperature study of $\beta\beta$DNP, the nonviscous activation energy E_b was found to equal 2.86 kcal/mol.[55] Since $\beta\beta$DNP is expected to have a lower hindrance to segmental motion than the P2VN sample, it is concluded that all the compounds are describable by this theory.

On the basis of Kramers' results,[44] the rate of excimer formation after a single hindered rotation in the dimer is predicted to have the following form in the "intermediate-friction" regime:

$$k_{rot} = \frac{1}{\xi}\left[\frac{f_p(k_ak_b)^{1/2}}{\pi}\right] \times \left[\frac{1}{1 + (1 + 4k_bM/\xi^2)^{1/2}}\right] \exp\left(-\frac{E_b}{R_gT}\right) \tag{15}$$

where ξ is the local friction factor and f_p is the fraction of passages by an excited chromphore over the barrier which lead successfully to excimer formation. For diffusion-controlled photophysics, eq 15 is substituted into eq 4 for dimer compounds to yield

$$R = \frac{1}{\xi}\left[\frac{Ek_{FD}}{k_{FM}(k_{FD} + k_{ID})}\right] \times \left[\frac{f_p(k_ak_b)^{1/2}}{\pi}\right]\left[\frac{1}{1 + (1 + 4k_bM/\xi^2)^{1/2}}\right] \exp\left(-\frac{E_b}{R_gT}\right) \tag{16}$$

Note that since there is no energy migration possible in the dimer, the enhancement factor E equals unity.

The limiting behavior of eq 16 with regard to the magnitude of the term $4k_bM/\xi^2$ is of particular interest. In the low-friction limit, $4k_bM/\xi^2 \gg 1$ and eq 16 may be written

$$R\eta = \frac{k_b^{1/2}C_1\eta}{2k_b^{1/2}M^{1/2} + \xi} \tag{17}$$

where

$$C_1 = \frac{E}{\pi}\frac{k_{FD}}{k_{FM}}\tau_D f_p k_a^{1/2} \exp(-E_b/R_gT)$$

In the high-friction limit, on the other hand, $4k_bM/\xi^2 \ll 1$ and eq 16 becomes

$$R\eta = \frac{k_b^{1/2}C_1\eta}{2\xi} \tag{18}$$

The Kramers treatment should be directly applicable to the model compound, where rotation involves a single

degree of freedom. Skolnick and Helfand[51] have extended Kramers' theory in the high-friction limit to many degrees of freedom in order to obtain an expression applicable to polymers. Their result is of the form

$$k_{rot} = \frac{C_2}{\xi} \exp\left(-\frac{E^*}{R_g T}\right) \tag{19}$$

where E^* is the energy of the multidimensional saddle point which must be surmounted and C_2 contains configurational factors which should not be affected by pressure. The factors making up C_2 include functions of the moments of inertia, the determinant of the potential matrix, and the eigenvalue for the direction of steepest descent from the saddle point. An expression for $R\eta$ for the polymer which is analogous to eq 18 for the dimer may then be obtained as

$$R\eta = C_3 \frac{\eta}{\xi} \exp\left(-\frac{E^*}{R_g T}\right) \tag{20}$$

where C_3 is a constant.

Further analysis of eq 16–20 requires that the form of the local friction coefficient ξ be specified. The simplest expression is that arising from the Stokes formalism

$$\xi_S = 6\pi\eta r \tag{21}$$

where η is the bulk solvent viscosity and r is the equivalent spherical radius of the diffusing particle. Substitution of ξ_S for ξ in the low-friction-limit expression, eq 17, leads to an expression which has the same form as the internal viscosity model, eq 8b, with $A_2 = 2M^{1/2}/C_1$ and $A_3 = 6\pi r/C_1 k_b^{1/2}$. This result is particularly interesting because it provides insight into the nature of the two contributions to the internal viscosity. In the high-friction limit, under conditions of Stokes diffusion

$$R\eta = C_1 k_b^{1/2}/12\pi r \tag{22}$$

and the intermolecular diffusion result, eq 6, is reproduced. Finally, application of the Stokes formalism to the intermediate-friction regime represented by eq 16 leads to

$$R\eta = \frac{C_1 k_b^{1/2}}{6\pi r}\left[\frac{1}{1 + [1 + 4k_b M/(6\pi\eta r)^2]^{1/2}}\right] \tag{23}$$

which displays concave-downward curvature on a plot of $R\eta$ vs. η.

The Kramers treatment presumes that the rotational diffusion will depend more upon the presence of the internal barrier to rotation than upon the volumetric requirements. If, on the other hand, transport is limited by the availability of free volume, the local friction factor relevant to the segmental motion leading to excimer formation may not be the same as that for the viscous transport of solvent molecules past one another. In other words, the effective or microscopic viscosity sensed by the excimer probe may differ from the macroscopic solvent viscosity. Since the high-friction limit of the hindered rotation model has been posited as describing the motions for polymers, this concept will be tested using that simplification.

At constant temperature, eq 18 may be written in the form

$$R\eta = A_5'(\xi_1/\xi_2) \tag{24}$$

where A_5' is a constant, ξ_1 is the friction factor applicable to viscous transport of solvent molecules in the pure solvent, and ξ_2 is the friction factor applicable to the trans–gauche rotation associated with intramolecular excimer formation in solution. Clearly, if the two processes are physically identical, $\xi_1 = \xi_2$ and $R\eta$ will be constant. It appears that this is the situation for intermolecular excimer formation.

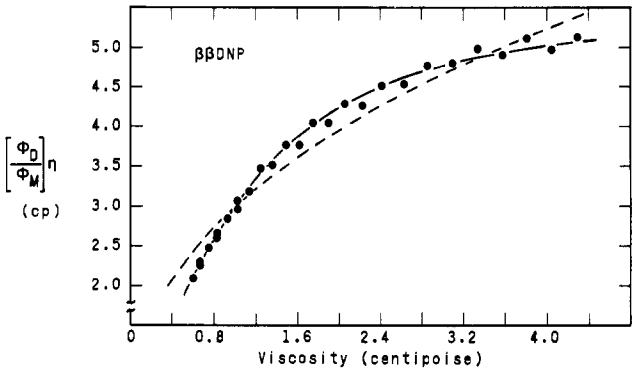

Figure 7. Comparison of experimental results for ββDNP with the best fits of the hindered rotation model in the intermediate-friction region (solid line) and the free volume limited model in the high-friction limit (dashed line).

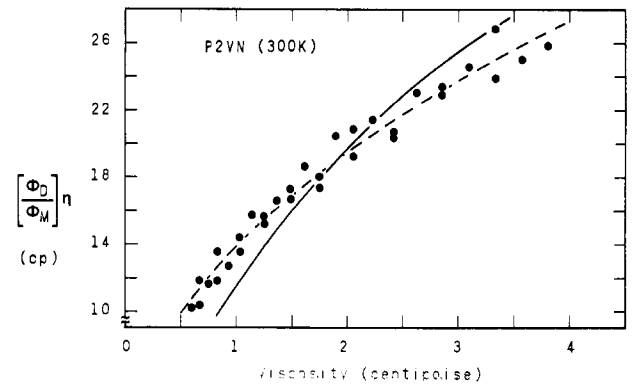

Figure 8. Comparison of experimental results for P2VN(300 000) with the best fits of the hindered rotation model in the intermediate-friction region (solid line) and the free volume limited model in the high-friction limit (dashed line).

If transport is limited by the availability of free volume, however, intermolecular and intramolecular processes might be expected to be appreciably different. This may be treated most simply by assuming that ξ_1 and ξ_2 are both proportional to viscosities which may be represented by Doolittle expressions having different values of γ. Applying eq 9 yields

$$R\eta = A_5 \exp\left(\frac{\gamma_1 - \gamma_2}{V_f}\right) \tag{25}$$

where γ_1 is the effective volume required for viscous transport, γ_2 is the effective volume required for a trans–gauche rotation, and A_5 is a constant.

Substituting eq 9 for η in eq 11a yields

$$R\eta = A_2\eta_0 \exp(-\beta\gamma_1/V_f) \tag{26}$$

A comparison of eq 25 with the empirical expression of eq 26 leads to the conclusion that $\gamma_2 = \gamma_1\beta$. If the effective volume required for the viscous interchange of positions in the pure solvent is the same as for the segmental rotation, $\gamma_1 = \gamma_2$ and $\beta = 1$. If $\beta < 1$, however, less volume is required for the intramolecular motion than for the corresponding intermolecular translation.

D. Comparison with Experiment. Figures 7 and 8 present the experimental viscosity dependence of $R\eta$ for ββDNP and P2VN(300 000). In each case, the solid line represents the best least-squares fit of the data to the general expression for the hindered rotation model in the intermediate-friction regime, eq 23. This should be valid

Table II

	hindered rotation			free volume limited	
	$C_1/6\pi r$	k_b, N/m	$\omega_b \times 10^{-13}$ s^{-1}	A_4	β
$\beta\beta$DNP	0.232	2255	2.21	0.762	0.612
P2VN(300 000)	0.959	3510	2.75	13.8	0.511

for the $\beta\beta$DNP dimer, for which it was derived, but should only be an approximation for the polymer which has a considerably more complex potential energy surface. Nevertheless, forcing the polymer data into this form provides a means for qualitatively comparing the effect of adjacent neighbor interactions on the dyad interconversion. A dashed line on these figures represents the best fit of the free volume limited model, eq 11a. Both models have two adjustable parameters: C_1 and k_b (hindered rotation) and A_4 and β (free volume limited). These are tabulated in Table II along with the calculated vibrational frequency at the barrier maximum, ω_b. Here the equivalent radii of a methylene-substituted naphthyl group and a toluene molecule were calculated by using the group contribution method of Bondi.[56]

Before comparing these results to previous experiments, some brief observations on the magnitude of the fitting constants are in order. First, an independent estimate of ω_b may be obtained if each oscillation is considered analogous to an encounter in the theory of absolute reaction rates. The universal frequency factor in such a case is kT/h, where k is Boltzmann's constant and h is Planck's constant. At 30 °C, the value of this factor is 6.32×10^{12} s^{-1}, which is of the same order as the ω_b values in Table II. Thus, the numerical value is at least reasonable.

Second, the major source of variability in both A_4 and $C_1/6\pi r$ is the inclusion of energy migration in the polymer sample which is, of course, absent in the dimer. If all of the change were attributed to variation in E, the hindered rotation model would lead to an E value of 4.1 for P2VN(300 000) whereas the free volume limited model leads to an E value of 18 for P2VN(300 000).

Based upon a goodness-of-fit criterion, it is apparent from the results of Figure 7 that excimer formation in $\beta\beta$DNP is better described by the hindered rotation model. With a similar degree of certainty, the P2VN(300 000) sample is better described by the free volume limited model. Since the transition from the hindered rotation to free volume limited cases coincides with the increasing chain length, it appears that intramolecular steric interactions have a significant effect on the ease of segmental motion associated with excimer formation.

Summary

Excimer formation resulting from intramolecular rotational diffusion of backbone segments in $\beta\beta$DNP and P2VN has been shown to deviate significantly at low viscosities from the prediction of Stokes diffusion for the intermolecular process. Previous attempts to explain this deviation have focused either on the importance of internal barriers to the motion or on the volumetric requirements. If the volumetric requirements for segmental diffusion are comparable to those for the solvent motion, the Kramers hindered rotation model developed in this work provides a means of treating the range of behavior possible. This model reduces to the internal viscosity result in the low-friction limit and to the intermolecular result in the high-friction limit. The flexible $\beta\beta$DNP is shown to be fit quite well by the hindered rotation model in the intermediate-friction regime. On the other hand, the more sterically hindered P2VN is better described by assuming high-friction-limit behavior, with the available free volume being the limiting factor.

In subsequent papers in this series, the structure of the diffusing segment as well as the solvent and temperature will be varied in order to assess more quantitatively the relative contributions of the hindered rotation and free volume limited diffusion processes.

Acknowledgment. This work was supported in part by the Institute for Energy Studies at Stanford University and in part by the Petroleum Research Fund, administered by the American Chemical Society. The high-pressure optical cell and hydraulic system were designed and assembled by C.W.F. while employed by Sandia National Laboratories. The authors thank Dr. Larry Harrah of Sandia for the loan of the pressure apparatus for this work. In addition, thanks are given to Dr. Ralph Trujillo, also of Sandia, for the synthesis of the $\beta\beta$DNP.

References and Notes

(1) Birks, J. B. "Photophysics of Aromatic Molecules"; Wiley-Interscience: New York, 1970.
(2) Birks, J. B. *Prog. React. Kinet.* **1970**, *5*, 181.
(3) Klöpffer, W. In "Organic Molecular Photophysics"; Birks, J. B., Ed.; Wiley-Interscience: New York, 1973.
(4) Johnson, G. E. *J. Chem. Phys.* **1975**, *63*, 4047.
(5) Avouris, P.; Kordas, J.; El-Bayoumi, M. A. *Chem. Phys. Lett.* **1974**, *26*, 373.
(6) Wang, Y. C.; Morawetz, H. *J. Am. Chem. Soc.* **1976**, *98*, 3611.
(7) Goldenberg, M.; Emert, J.; Morawetz, H. *J. Am. Chem. Soc.* **1978**, *100*, 7171.
(8) Liao, T. P.; Yokamoto, Y.; Morawetz, H. *Macromolecules* **1979**, *12*, 535.
(9) Förster, Th.; Leiber, C. O.; Seidel, H. P.; Weller, A. *Z. Phys. Chem. (Frankfurt am Main)* **1963**, *39*, 265.
(10) Seidel, H. P.; Selinger, B. K. *Aust. J. Chem.* **1965**, *18*, 977.
(11) Braun, H.; Förster, Th. *Ber. Bunsenges. Phys. Chem.* **1966**, *70*, 1091.
(12) Speed, R.; Selinger, B. *Aust. J. Chem.* **1969**, *22*, 9.
(13) Johnson, P. C.; Offen, H. W. *J. Chem. Phys.* **1971**, *53*, 2495.
(14) Braun, H.; Förster, Th. *Z. Phys. Chem. (Frankfurt am Main)* **1972**, *78*, 40.
(15) Johnson, P. C.; Offen, H. W. *J. Chem. Phys.* **1972**, *56*, 1638.
(16) Johnson, P. C.; Offen, H. W. *Chem. Phys. Lett.* **1973**, *18*, 258.
(17) Johnson, P. C.; Offen, H. W. *J. Chem. Phys.* **1973**, *59*, 801.
(18) Chandross, E. A.; Dempster, C. J. *J. Am. Chem. Soc.* **1970**, *92*, 3586.
(19) Parker, C. A. "Photoluminescence of Solutions"; Elsevier: Amsterdam, 1968.
(20) Bard, Y. "Nonlinear Parameter Estimation"; Academic Press: New York, 1974.
(21) Marquardt, D. W. *J. Soc. Ind. Appl. Math.* **1963**, *11*, 431.
(22) Yakhot, V.; Cohen, M. D.; Ludmer, E. *Adv. Photochem.* **1979**, *11*, 489.
(23) Flory, P. J. "Statistical Mechanics of Chain Molecules"; Interscience: New York, 1969.
(24) Frank, C. W.; Harrah, L. A. *J. Chem. Phys.* **1974**, *61*, 1526.
(25) Bovey, F. A.; Hood, F. P.; Anderson, E. W.; Snyder, L. C. *J. Chem. Phys.* **1965**, *42*, 3900.
(26) Johnson, L. F.; Heatley, F.; Bovey, F. A. *Macromolecules* **1970**, *3*, 175.
(27) Yoon, D. Y., private communication.
(28) Yoon, D. Y.; Sundararajan, P. R.; Flory, P. J. *Macromolecules* **1975**, *8*, 776.
(29) Nishijima, Y.; Yamamoto, M. *Polym. Prepr., Am. Chem. Soc., Div. Polym. Chem.* **1979**, *20*, 391.
(30) Zachariasse, K. A., private communication.
(31) W. Klöpffer provided an excellent review as part of the Eighth Aharon Katzir-Katchalsky Memorial Conference on "Luminescence from Macromolecules—Biological and Synthetic", June 1980 (to be published in *Ann. N.Y. Acad. Sci.*, 1981).
(32) Zachariasse, K. A.; Kühnle, W.; Weller, A. *Chem. Phys. Lett.* **1978**, *59*, 375.
(33) Stevens, B.; Ban, M. I. *Trans. Faraday Soc.* **1964**, *60*, 1515.
(34) Aladekomo, J. B.; Birks, J. B. *Proc. R. Soc. London, Ser. A* **1965**, *284*, 551.
(35) Hamilton, T. D. S.; Naqvi, K. R. *Chem. Phys. Lett.* **1968**, *2*, 374.
(36) Al-Wattar, A. H.; Lumb, M. D. *Chem. Phys. Lett.* **1971**, *8*, 331.

(37) Sambursky, S.; Wolfsohn, G. *Phys. Rev.* **1942**, *62*, 357.
(38) McRae, E. G. *J. Phys. Chem.* **1957**, *61*, 562.
(39) Weigang, D. E. *J. Chem. Phys.* **1960**, *33*, 892.
(40) Robertson, W. W.; King, A. D. *J. Chem. Phys.* **1961**, *34*, 1511.
(41) Skinner, J. F.; Cussler, F. L.; Fuoss, R. M. *J. Phys. Chem.* **1968**, *72*, 1057.
(42) Stevens, B.; Dickenson, T. *J. Chem. Soc.* **1936**, 5492.
(43) Peterlin, A. *J. Polym. Sci., Polym. Lett. Ed.* **1972**, *10*, 101.
(44) Kramers, H. A. *Physica* **1940**, *7*, 284.
(45) Doolittle, A. K. *J. Appl. Phys.* **1951**, *22*, 1471.
(46) Gegiou, D.; Muszkat, K. A.; Fisher, E. *J. Am. Chem. Soc.* **1968**, *90*, 12.
(47) Bokobza, L.; Jasse, B.; Monnerie, L. *Eur. Polym. J.* **1980**, *16*, 715.
(48) Helfand, E. *J. Chem. Phys.* **1971**, *54*, 4651.
(49) Helfand, E. *J. Chem. Phys.* **1978**, *69*, 1010.
(50) Helfand, E.; Wasserman, Z. R.; Weber, T. A. *Macromolecules* **1980**, *13*, 526.
(51) Skolnick, J.; Helfand, E. *J. Chem. Phys.* **1980**, *72*, 5489.
(52) Blomberg, C. *Chem. Phys.* **1979**, *37*, 219.
(53) Weber, T. A. *J. Chem. Phys.* **1979**, *70*, 4277.
(54) Iwata, K. *J. Chem. Phys.* **1973**, *58*, 4184.
(55) Frank, C. W.; Fitzgibbon, P. D., unpublished results.
(56) Bondi, A. *J. Phys. Chem.* **1964**, *68*, 441.

Mean Field Theory of Polymer Solutions: Concentration Dependence of Chain Dimensions

D. J. Lohse

Exxon Chemical Company, Elastomers Technology Division, Linden, New Jersey 07036.
Received July 31, 1981

ABSTRACT: A mean field theory for an incompressible polymer solution on a lattice is presented. Both excluded volume and attractive (van der Waals) interactions are included. The central concept is that of a screening length, x_s. Configurations of a chain which are larger than x_s have complete screening due to overlap with neighboring chains and so they have the statistics of ideal chains. Configurations smaller than x_s experience no overlap and thus have the statistics of isolated chains. The results of this model are developed in terms of the concentration dependence of the chain dimensions. These results are similar to, but in detail different from, the results of the recent scaling theories.[1-7] Chain dimensions show a power law relation with concentration in the semidilute region, but the power depends on molecular weight. Also, a slight expansion of chains in dilute Θ solutions is predicted. The agreement of these results with experiment is good.

I. Introduction

The statistical mechanics of polymer solutions have presented a challenge for scientists for well over 40 years. Even when considered as single chains, the polymer problem has not been solved exactly. Because the chains are long, an immense number of configurations are available to them. The enumeration of them is made more difficult because the chain cannot pass through itself—such hard-core repulsions give rise to the excluded volume effect. On top of this there are attractive, secondary forces (van der Waals) between chain segments as well as with the solvent. Such consideration of a single chain has application in dilute solutions in which the chains are essentially isolated from each other. However, the complexity becomes more severe when more than one chain is considered, that is, when the effects of concentration are included. At some point the region of space in which the segments of a chain are found will coincide with that of one or more other chains. Thus, the sizes of the coils will determine what interactions they experience. But these interactions will in turn influence the chain sizes. Such overlapping may cause the coils to contract away from one another (in good solvent) or to expand toward one another (in poor solvent). Those cases for which there is some overlap between chains, as well as some isolation, are called semidilute solutions, which have proved difficult to handle.

In the past decade, renewed interest in polymer solutions has been stimulated by both theoretical and experimental advances. Scaling theories, based on the renormalization group techniques used in the theory of phase transitions and critical phenomena, have been developed for single chains by de Gennes[1] and extended to semidilute solutions by des Cloizeaux[2] and Daoud and Jannink.[3,4] Such theories have also been derived recently by Kosmas and Freed[5] without the use of renormalization techniques. Good general reviews of these theories may be found in ref 6 and 7. Central to these developments is the concept of a screening length, first introduced by Edwards.[8] For distances shorter than the screening length, the intramolecular forces still have full effect, but at larger distances their effect is screened out by interactions with segments from other chains. As a result, power law expressions for chain dimensions and other functions can be determined.

The excitement generated by the new theories was partly due to the agreement they have had with the new experimental technique of small-angle neutron scattering (SANS). In order to see a single chain in a sea of similar chains (as in the bulk state or in semidilute and concentrated solutions) it is necessary to label the chain in some way. Photon scattering (light and X-ray) is due to electromagnetic forces, so the internal structure of a sample is seen by contrasts in electron density (X-ray) or polarization (light). But any labeling technique that causes a significant contrast in electron density (e.g., by attaching iodine to polystyrene[9]) also causes chemical changes, and so the labeled chain is no longer representative of the unlabeled chains. Neutrons are scattered, primarily, by interactions with the nuclei of the sample.[10] Isotopes of the same element may thus have different scattering properties, of which the most common example is the great difference in neutron scattering cross section between hydrogen and deuterium. When isotopic labeling is used, there should be no large chemical differences. Thus, for the first time, measurements of single-chain properties in concentrated systems have become possible.[11]

The theory presented here is based on mean field concepts. One basis is the seminal work of Flory[12] and Huggins[13] on polymer solutions, as well as later extensions of this approach.[14-16] Since fluctuations in segment density are not included in these theories, they work best in con-

0024-9297/81/2214-1658$01.25/0